



Design and Development of an MRI Compatible Circuit Suitable for Pre-Clinical Physiological Monitoring in a 4.7T Magnetic Resonance Imaging

B. E. Eze ^{a*}, N. A. Akonjom ^a and A. E. Bassey ^b

^a Department of Physics, Cross River University of Technology, Calabar, Nigeria.

^b Department of Sociology (Medical), University of Calabar, Calabar, Nigeria.

Authors' contributions

This work was carried out in collaboration among all authors. All authors read and approved the final manuscript.

Article Information

DOI: 10.9734/AJOPACS/2023/v11i2196

Open Peer Review History:

This journal follows the Advanced Open Peer Review policy. Identity of the Reviewers, Editor(s) and additional Reviewers, peer review comments, different versions of the manuscript, comments of the editors, etc are available here: <https://www.sdiarticle5.com/review-history/98258>

Original Research Article

Received: 01/02/2023
Accepted: 03/04/2023
Published: 14/04/2023

ABSTRACT

As monitoring preclinical MRI is essential, it is important that the equipment used must be MRI-compatible. This is because interaction with an MRI radiofrequency (RF) transmitting field can cause RF burns due to inappropriate equipment. And non-compatible MRI monitoring equipment can give inaccurate readings in the MRI system if the equipment has ferromagnetic components. Preclinical MRI is designed for animals, the model used to study diseases related to humans. Animal models are imaged using a smaller scanner with high magnetic fields like the 4.7T. The main parameters of interest are the respiratory rate, the temperature, the pressure transducer and the electrocardiogram (ECG), this is because the animal model is used as a laboratory experiment for human disease. An MRI-compatible lead II ECG simulator, with approximately 0.5 mV output amplitude was attached to the input of the ECG preamplifier to represent a small animal's signal. The transmitted signal is the ECG, the pressure sensor, the temperature, and the battery (voltage),

*Corresponding author: E-mail: ezebenson1@gmail.com;

these are all linked to different channels (outside, near and inside magnet) and were acquired with the pressure sensor pad taped on a male adult volunteer's thumb to record the human pulse of 70 bpm, which is similar to the respiration rate of an anaesthetized mouse or rat. The use of a signal gating generator should be explored in future work, this could make the monitoring parameters to be independent of the RF pulse influence. Finally, fibre optics should be included in the design process.

Keywords: MRI; ECG; compatible; physiological monitor; preclinical; temperature; pressure sensor; respiratory sensor.

1. INTRODUCTION

Physiological monitoring for preclinical magnetic resonant imaging (MRI), is designed to mainly meet the physiological monitoring and gating requirement for anaesthetizing small rodents such as rats and mice, and even larger animals in an MRI setting. The major benefits of the MRI is excellent in soft tissue contrast and also has the ability to image 3-D structure and function in high inter-session replicate [1].

Preclinical MRI is used for studying small animals such as rodents to understand the pathophysiology of various diseases, develop and test new therapies, and evaluate the efficacy of drugs [2]. During the MRI scan, animals may experience stress and anxiety, which can cause changes in their physiological parameters, such as heart rate, respiratory rate, blood pressure, and body temperature. These changes can affect the quality of the MRI data obtained and result in inaccurate measurements [3].

Preclinical MRI is designed for animals, a model used to study diseases related to humans. Animal models are imaged using a smaller scanner with a high magnetic field like the 4.7T [4]. Neurological situations, for diseases of the joints and muscles, for assessing tumors, and also used for showing abnormalities in the heart and blood cells. Modern clinical whole-body MRI scanner has a magnetic field strength range from 0.5T-3.0T [5].

This research work is mainly Centre on pre-clinical MRI scanners, because, the animal model used widely is based on pre-clinical scanners owing to the substantial benefits in the quality of image acquisition, sensitivity, and spatial resolution, that can be acquired using a smaller scanner with a high magnetic field like the 4.7T. As rat and mouse brains are about 3,000 times much smaller compare to the brain of humans, the pre-clinical scanner is necessary to achieve high resolution [6].

In physiological monitoring of basic parameters such as temperature, respiration, heartbeat and electrocardiogram (ECG) for small animals such as rats and mice to remain still throughout the period of the MRI examination, a general anaesthetic is required to acquire decent high-quality MRI images. As monitoring preclinical MRI is essential, it is important that the equipment used must be MRI-compatible. [7].

1.1 Theoretical Background

It is widely known that physiological monitoring for preclinical MRI is achieved using a high field magnets B_0 with a very small bore specifically designed for rodents (rats and mice) [8]. The B_0 is a static magnetic field, and the significance of using the high magnetic field (B_0) is the high resolution that is achieved due to the increase in signal, as a result of increased sample magnetization caused by a greater number of aligned spins from the Boltzmann distribution and the increased Faraday induction from the higher frequency given as;

$$fL = \left(\frac{\gamma}{2\pi}\right)B_0 \quad (1)$$

Where γ is gyromagnetic, fL is the Larmor frequency and B_0 is the magnetic field.

Usually, preclinical uses a higher magnetic field B_0 range of 4.7T to 7T. For the purpose of this project magnetic field of 4.7T (200 MHz) is used [9].

Preclinical MRI is designed for animals, the model used to study diseases related to humans. Animal models are imaged using a smaller scanner with high magnetic fields like the 4.7T. Neurological situations, for diseases of the joints and muscles, for assessing tumours, and also used for showing abnormalities in the heart and blood cells. Modern clinical whole-body MRI scanner has a magnetic field strength range from 0.5T-3.0T [10].

The magnetic dipole moment μ in the classical moment experiences a torque L , that will align with the magnetic field B_0 was given as

$$L = \mu \times B_0 \quad (2)$$

As the nucleus also has angular momentum p , the nucleus precesses because of the torque around the magnetic field B_0 , relatively, similar to a gyroscope in a gravitational field. The angular momentum changing rate is given as:

$$\frac{dp}{dt} = L = \mu \times B_0 \quad (3)$$

and from the equation (2), $\mu = \gamma p$, then

$$\frac{du}{dt} = u \times \gamma B_0 \quad (4)$$

where γ is the gyromagnetic ratio, and the Larmor frequency is given as:

$$\omega L = -\gamma B_0 \quad (5)$$

Eqn. (4) and (5), show the direction of the applied field at which the nucleus precesses, at ω rad/s, and the negative sign indicates the direction of rotation. The resonant frequency is known as the Larmor frequency.

MRI rely on the process called nuclear magnetic resonant (NMR) which is the way atomic nuclei interacted with an externally applied magnetic field. It can be achieved through any type of nucleus, as long as it is a non-zero spin indicated by $I \neq 0$, and has angular momentum aligned with the spin axis [11] as

$$p = \hbar I \quad (6)$$

Where I is the spin, \hbar is the Plank constant given as $\hbar = h/2\pi$

2. METHODOLOGY

The reason why main parameters of interest in this research are the respiratory rate, the temperature, the pressure transducer and the electrocardiogram (ECG), this is because the animal model is used as a laboratory experiment for human disease.

The temperature sensor used was a chip thermistor with dimensions x mm, y mm, z mm (NTCS0603E3103JHT, Vishay, US) [12], with b value of 3960K, tolerance of $B_{25/85} = \pm 1$, and R_{25}

value of 10k Ω from equation (1). The thermistor obeys the exponential law.

$$R = Ae^{(b/T)} \quad (7)$$

Where b is the constant temperature in Kelvin (K), and depends on the composition; 3000 – 4000K, the value within the datasheet and A is in (Ω) depending on the sensor shape. Supplied with calibration value of R_0 at T_0 which allows the elimination of A from equation (7) to give

$$R = R_0 e^{b(1/T - 1/T_0)} \quad (8)$$

Where R is the unknown resistance, R_0 is the calibrated resistance, $1/T$ is the unknown temperature and $1/T_0$ is the calibrated temperature.

The pressure transducer's datasheet is, Freescale; MPX5100AP/GP pressure transducer with Graseby sensor pad, used for respiration. It is an on-chip condition integrated silicon pressure sensor, suitable for microcontrollers or microprocessors. The MPX5100 is a piezoresistive transducer series.

The abdominal respiratory sensor used is a small pressure pad designed for infant apnoea alarms (MRI0, Graseby, UK). A small volume of air passes through the sensor tube to the monitor, caused by the expansion of the abdominal wall during breathing. Other components datasheet used are; LM285Z – 2.5V reference, and TC 7660S Charge pump (negative voltage generator) [13].

The ECG preamplifier uses an instrumentation amplifier as the input stage. (INA118, Texas Instrument, USA) [14]. It is made up of three operational amplifiers, seven resistors arranged to give a differential gain stage with a good common mode rejection ratio and a high input impedance. Six of the resistors and the three op-amps are connected to an 8-pin package of the INA118 instrumentation amplifier chip.

The gain of the INA118 instrumentation amplifier is set at the input stage by using an external resistor R_G to a value given as;

$$G = 1 + 50k\Omega/R_G \quad (9)$$

The choice for the gain is to boost the ECG output signal level to about 1 V, and the gain for an R_G value of 50 ohms was calculated to be 1001.

First among the measurement was the thermistor designed to be inserted inside the body of the animal to determine the body temperature. The negative temperature coefficient (NTC) thermistor was soldered to a twisted pair of 0.2 mm enameled copper wires to allow resistance measurements. The thermistor was temporarily glued to a copper block of approximate dimensions of 5 mm x 20 mm x 40 mm to which a silicon temperature sensor with a 10 mV/°C output (LM35, Texas Instrument, USA) [15], was also attached. The copper block was heated up to approximately 40°C by applying a lot of soldering iron for a few seconds, and then was placed on a polystyrene block and covered so that it cooled to room temperature over a period of several minutes. Copper has high thermal conductivity and a high heat capacity, so this helps the thermistor and reference sensor at the same temperature during cooling. The measurement of resistance versus temperature shows that as temperature increases it led to a decrease in resistance.

A signal generator (Gwinstek, SFG-1013, China) was used to generate a sign wave signal of amplitude approximately 1 V at a frequency between 1 Hz and 120 Hz and this was applied to the input of the ECG preamplifier via a 1000:1 potential divider to reduce the amplitude to the level of an ECG R-wave. The amplitude of

the output and input voltages were recorded using an oscilloscope (Tenma colour signal, Tenma Testing Equipment, USA) and the transfer function $|T(f)|$ was calculated from the ratio and plotted against frequency as seen in Fig. 1.

3. RESULTS AND DISCUSSION

The physiological sensors and signal processing circuits were tested in the MRI system. An MRI-compatible lead II ECG simulator, with approximately 0.5 mV output amplitude was attached to the input of the ECG preamplifier to represent a small animal's signal as shown in Fig. 1.

The fitted line shows that when operated in the voltage-biased circuit, the thermistor response to temperature is more linear and has a sensitivity of approximately 30 mV/°C. The vertical dashed line indicates a normal body temperature of 37 °C.

A signal generator (Gwinstek, SFG-1013, China) was used to generate a sign wave signal of amplitude approximately 1 V at a frequency between 1 Hz and 120 Hz and this was applied to the input of the ECG preamplifier via a 1000:1 potential divider as seen in Fig. 2.

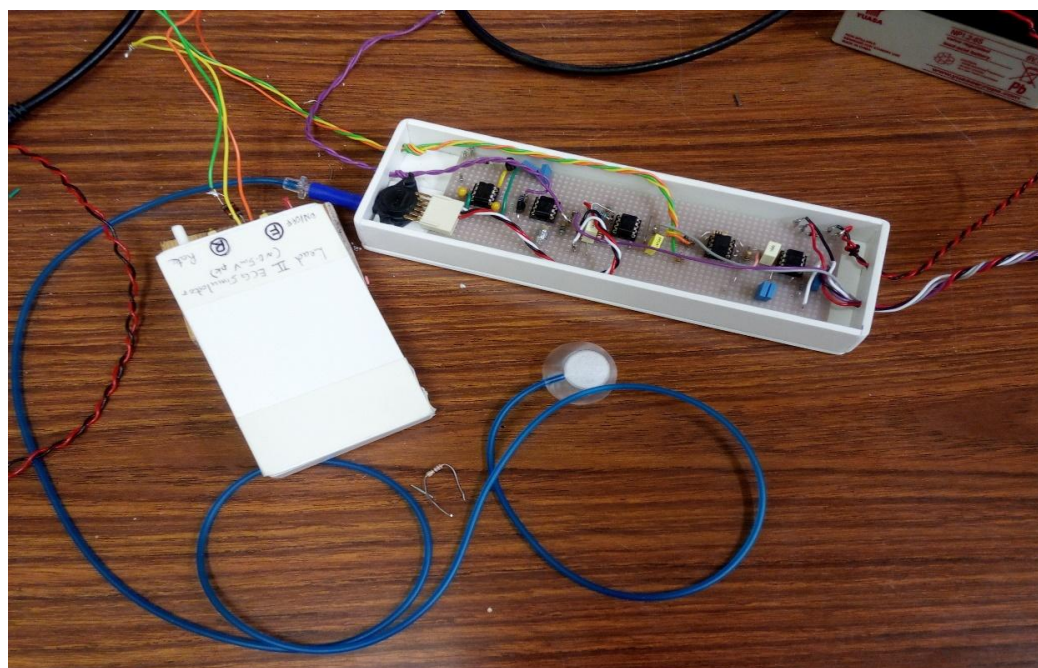


Fig. 1. ECG simulator connected to the circuit board, with the respiration pad attached to the silicon pressure sensor

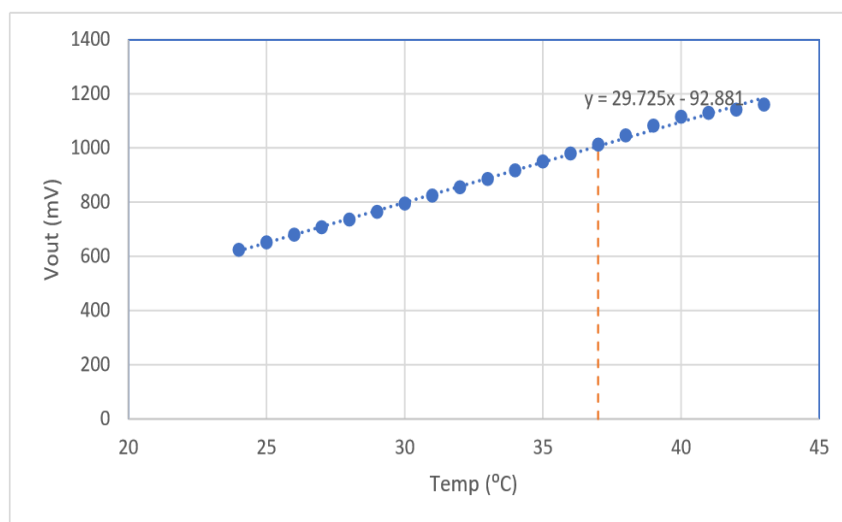


Fig. 2. Thermistor response versus temperature when operated with voltage bias and linearizing

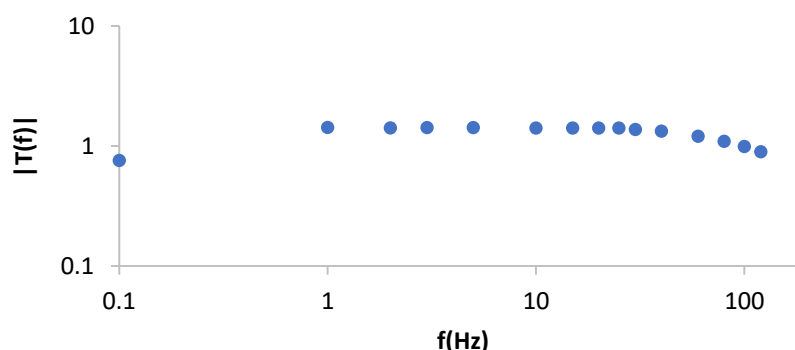


Fig. 3. The frequency response of the pressure sensor's preamplifier

The circuit board is then connected to a fibre optic link with a transmitter and a receiver, and the receiver is linked to a 12-bit ADC (1208FS, Measurement Computing, USA) and waveforms were captured using oscilloscope software (TracerDAQ, Measurement Computing, USA). The transmitted signal is the ECG, the pressure sensor, the temperature, and the battery (voltage), these are all linked to different channels as seen in Figs. 5-8. Figs. 5-7 (outside, near and inside magnet) were acquired with the pressure sensor pad taped on a male adult volunteer's thumb to record the human pulse of 70 bpm, which is similar to the respiration rate of an anaesthetized mouse or rat. Then Fig. 8 was acquired with the pressure sensor taped to the surface of a phantom to pick up vibration from the gradient system.

The calculated high pass cut-off frequency is 0.16Hz, while the cut-off frequency from the oscilloscope is 0.2Hz. The specific low pass cut-

off frequency is 100Hz, and the measured frequency from the oscilloscope is 99Hz. In this case, the output signal leads while the input signal lags behind, and there was a distortion in the waveform, as the amplifier tends to deliver higher output voltage, the waveform started clipping. Clipping is a situation where the output tends to go beyond the power supply rails which is not symmetrical. The gain and low characteristics of the pressure sensor as shown in Fig. 3.

The gradient echo measurements of the parameters were carried out to test interactions between the imager's RF and gradient pulses and physiological sensors. The tests used a gradient echo pulse sequence with a bandwidth of 50kHz, 256 x 256 pixels, slice thickness 1mm with a field of view (FOV) of 50mm. The gradient ramp time is 1000 μ s, the repetition time (TR) of 200ms, the echo time (TE) of 11ms and the flip angle of 45°.

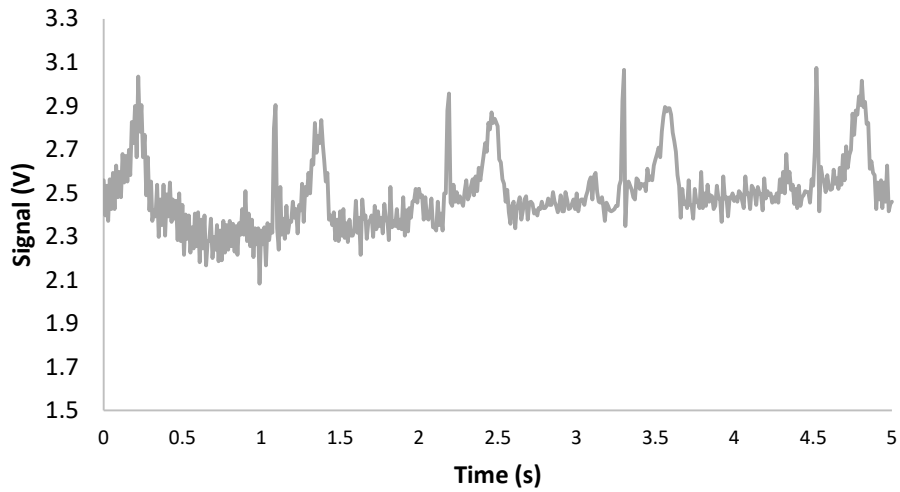


Fig. 4. The author's ECG

The author's ECG trace show noticeable 50Hz interference

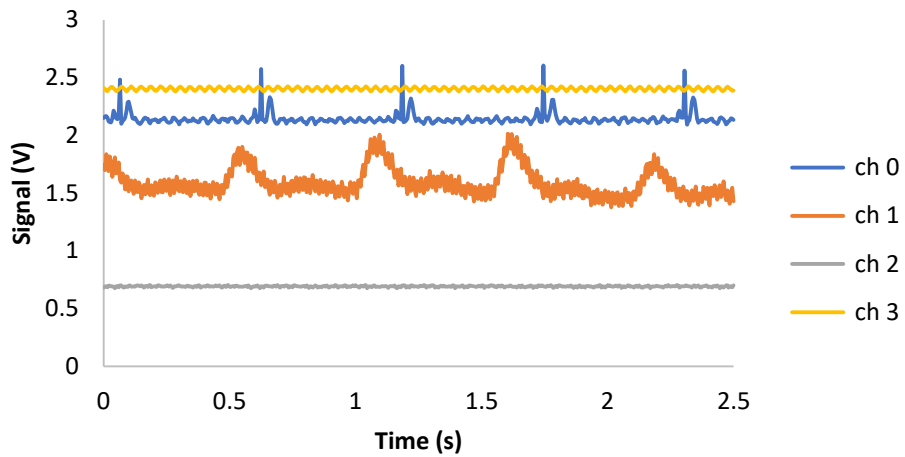


Fig. 5. Image inside the magnet

Channel 0: ECG, channel 1: pulse, channel 2: temperature and channel 3: battery voltage

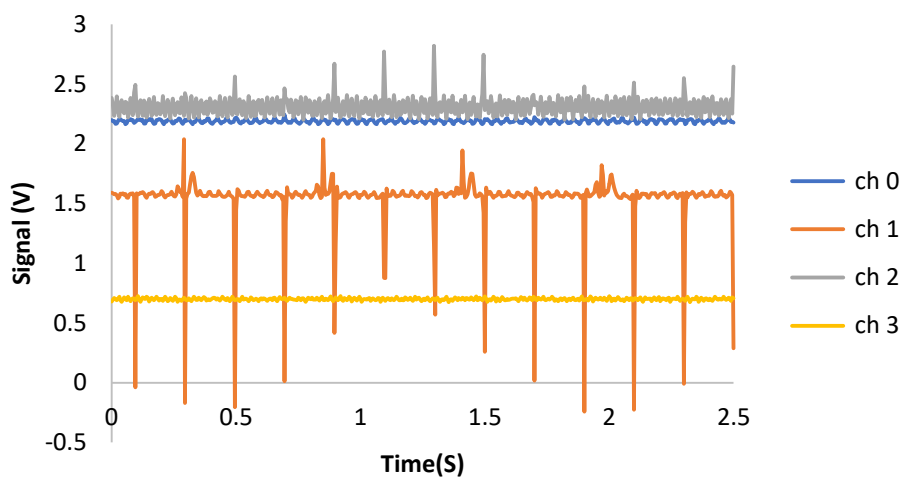


Fig. 6. Image outside magnet

Channel 0: battery voltage, channel 1: ECG, channel 2: vibration and channel 3: temperature

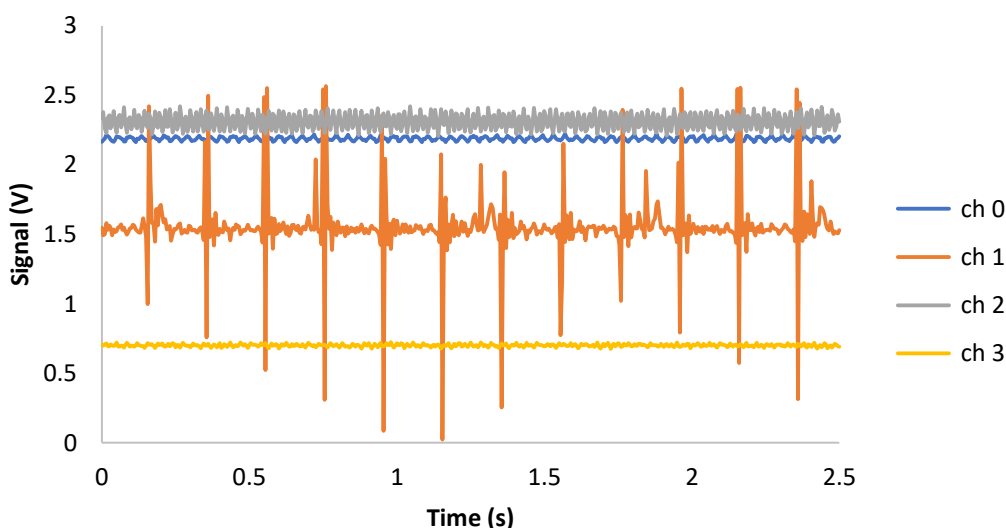


Fig. 7. Image near the magnet
Ch. 0: battery, ch. 1: ECG, ch. 2: Vibration, and ch. 3: temperature

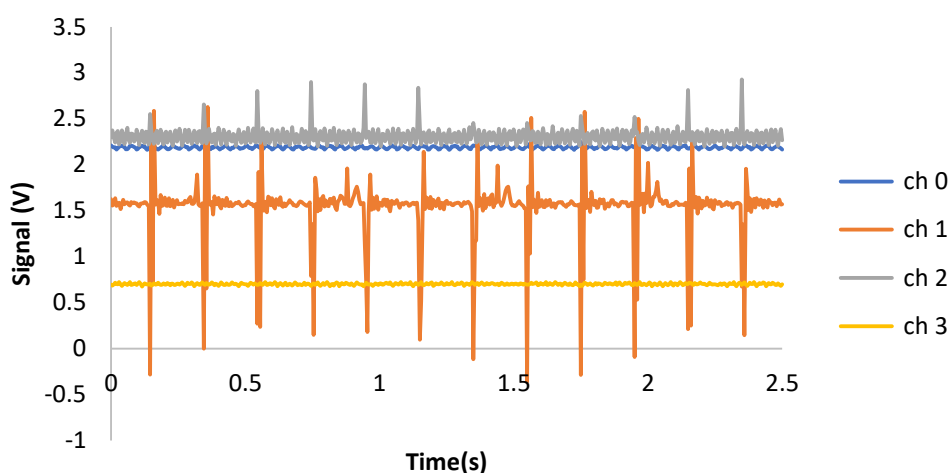


Fig. 8. Image with RF and gradient on
Ch.0: battery, ch. 1: ECG, ch. 2: vibration, ch.3: temperature

4. CONCLUSION AND RECOMMENDATION

Most of the components used are slightly ferromagnetic (i.e the resistors and the op-amps). The phantom show a high-quality image when the components were placed 20cm from the phantom as seen in Fig. 4 while in Fig. 6 where the circuit board was closed to the phantom, the image quality was so poor. The agarose gel phantom shows a high level of artefacts as compared to the water phantom with two thermistor chips. So, a water phantom with a small amount of NiSO₄ and a smaller thermistor chip were used for high-quality images and fewer artefacts.

The testing and measurement carried out in this project show that all the monitoring parameters do not perform as expected in the MRI system. The component's interaction with the MRI needs more research for MRI compatibility to be achieved. And nonferromagnetic components should be used.

The use of a signal gating generator should be explored in future work, this could make the monitoring parameters to be independent of the RF pulse influence as seen in Figs. 5-8. Finally, fibre optics should be included in the design process.

COMPETING INTERESTS

Authors have declared that no competing interests exist.

REFERENCES

1. Wesley D. Gilson, Dara L. Kraitichman. Magnetic resonance imaging in small rodents using clinical 1.5T and 3.0T scanners. *The Journal of Nuclear Medicine*. 2007;51(12):982-990.
2. Shrestha SS, Kotasidis FA, Zaidi H. "Recent advances in preclinical magnetic resonance imaging instrumentation and methodology." *Journal of Translational Imaging*. 2018;6(1):1-16.
3. Wehrl HF, Schwab J, Hasenbach K, Lerdkrai C, Claussen CD, Stiebellehner L. "Multimodal functional imaging of the hypoxic response after stroke." *Stroke*. 2015;46(6):1846-1852.
4. Lecomte R, Bénard F, Boisvert L, Cadorette J, Croteau E, Fontaine R, et al. "Preclinical PET/MRI: A new tool for small animal imaging." *Journal of Nuclear Medicine*. 2008;49(2):153 – 163.
5. Welch A, Mingarelli M, Riedel G, Platt B. "Mapping changes in mouse brain metabolism with PET/CT." *The Journal of Nuclear Medicine*. 2013;54(11):925-928.
6. Eze BE, Ushie PO, Ndifon KB. Physiological monitoring for pre-clinical magnetic resonance imaging. *International Journal of Scientific and Engineering Research*. 2018;9(11):1033-1038.
7. Vallee JP, Ivancevic MK, Nguyen D. Status of cardiac MRI in small animals; 2004.
8. Bartling SH, Kuntz J, Semmler W. Gating in small-animal cardio-thoracic CT. *Methods*. 2010;50:42–49.
9. Hadley JR, Payne JR. "A modular and scalable system for MRI-compatible physiological monitoring in small animals." *Magnetic Resonance in Medicine*. 2017;78(5):1921-1930.
10. Bloembergen, Purcell, Pound. Relaxation effects in nuclear magnetic absorption. *Phys. Revs*. 1948;73:679 – 712.
11. Datasheet. NTCS060E3103JHT, Vshay, Germany
12. LM 285Z – 2.5RAG 2.5V Reference, Texas Instrument, USA.
13. Freescale; MPX5100AP/GP.
14. INA118 Instrumentation amplifier datasheet.
15. LM35, Texas, Instrument, USA.

© 2023 Eze et al.; This is an Open Access article distributed under the terms of the Creative Commons Attribution License (<http://creativecommons.org/licenses/by/4.0>), which permits unrestricted use, distribution, and reproduction in any medium, provided the original work is properly cited.

Peer-review history:

The peer review history for this paper can be accessed here:

<https://www.sdiarticle5.com/review-history/98258>